

Supporting Information

Heterometallic Appended $\{MMn^{III}_4\}$ Cubanes Encapsulated by Lacunary Polytungstate Ligands

Hai-Hong Wu, Shuang Yao, Zhi-Ming Zhang,* Yang-Guang Li, You Song,*

Zhu-Jun Liu, Xin-Bao Han and En-Bo Wang *

CONTENTS

Section 1	Experimental Section
Section 2	Supplementary Structural Figures
Section 3	Magnetic properties
Section 4	Supplementary Physical Characterizations

Section 1 Experimental Section

1. Materials and Methods. All the reagents were commercially purchased and used without further purification. The $K_8[\gamma\text{-SiW}_{10}\text{O}_{36}]\cdot 12\text{H}_2\text{O}$ precursor was synthesized according to the literature^{S1} and characterized by IR spectrum. Elemental analyses (C and H) were performed on a PerkinElmer 2400 CHN element analyzer; Si, W, Mn, Dy, Sm, Er, K and Na were analyzed on a PLASMASPEC(I) ICP atomic emission spectrometer. IR spectra were recorded in the range 400-4000 cm^{-1} on an Alpha Centaur FTIR spectrophotometer using KBr pellets. TG analyses were performed on a Perkin–Elmer TGA7 instrument in flowing N_2 with a heating rate of 10 $^\circ\text{C}\cdot\text{min}^{-1}$.

2. Synthesis of 1: 0.51 g Dy_2O_3 was added in 10 mL distilled water, then 3.0 mL concentrated nitric acid was added in the mixture, which was refluxed for one hour resulting in solution A. 1.0 g $K_{12}[\gamma\text{-SiW}_{10}\text{O}_{38}]\cdot 12\text{H}_2\text{O}$ was dissolved in 30mL water, 1.0 g $\text{MnCl}_2\cdot 4\text{H}_2\text{O}$ (5.05 mmol) and 5 mL solution A were added, followed by addition of 1 mL morpholine and 15 ml 2 M K_2CO_3 aqueous solution. The resulting mixture with the pH value of 9.51 was further stirred at 60 $^\circ\text{C}$ for 4 h, Then 0.20 g NaCl was added into the resulting mixtures, which was further stirred for 10 min. Afterwards the solution was cooled down to ambient temperature and a brown residue was filtered off. After three days, brown tubular crystals suitable for X-ray diffraction were obtained (Yields: 27 % based on W). Anal. Found (%): C, 0.18; H, 0.93; Dy, 2.89; K, 4.99; Mn, 4.21; Na, 2.78, Si, 0.95; W, 55.61; Calcd: C, 0.23; H, 0.87; Dy, 3.06; K, 5.16; Mn, 4.14; Na, 2.60, Si, 1.06; W, 55.44. IR (KBr pellet): $\nu_{\text{max}}/\text{cm}^{-1}$

3433 (s), 1631 (s), 1461 (w), 1365 (w), 989 (w), 940 (w), 864 (m), 781 (m), 707 (m) and 507 (w).

Synthesis of 2. 1.0 g $K_{12}[\gamma\text{-SiW}_{10}\text{O}_{38}]\cdot 12\text{H}_2\text{O}$ was dissolved in 30 mL water, 1.0 g $\text{MnCl}_2\cdot 4\text{H}_2\text{O}$ (5.05 mmol) was added, followed by addition of 1 mL morpholine and 6 mL 2 M K_2CO_3 aqueous solution, the resulting mixture with the pH value of 9.99 was further stirred at 50 °C for 4 h. Then 0.20 g NaCl was added into the resulting mixtures, which was further stirred for 10 min. Afterwards the solution was cooled down to ambient temperature and a brown residue was filtered off. After two days, brown block crystals suitable for X-ray diffraction were obtained (Yield: 33 % based on W). Anal. Found (%): C, 0.17; H, 0.96; K, 7.27; Mn, 4.01; Na, 2.79; Si, 1.18; W, 55.67; Calcd: C, 0.23; H, 0.88; K, 7.43; Mn, 4.18; Na, 2.62; Si, 1.07; W, 55.91. IR (KBr pellet): $\nu_{\text{max}}/\text{cm}^{-1}$ 3430 (s), 1627 (s), 1459 (w), 1378 (w), 986 (w), 939 (m), 860 (s), 787 (m), 700 (s) and 503 (s).

3. X-ray Crystallography. The crystallographic data were performed on an Oxford Diffraction Gemini R CCD for **1**, and a Rigaku R-Axis RAPID IP diffractometer for **2**. The data were collected at 293 K, and graphite-monochromated Mo- $K\alpha$ radiation ($\lambda = 0.71073 \text{ \AA}$). The structures were solved by the direct method and refined by the Full-matrix least squares on F^2 using the SHELXL-97 software.^{S2} During the refinement of compounds **1** and **2**, all hydrogen atoms on water molecules and protonation were directly included in the molecular formula. The restraint command 'isor' was employed to restrain the oxygen atoms so as to avoid the ADP and NPD problems on them. This command leads to the restraint numbers 60 and 228 for the two

compounds, respectively. The crystal data and structure refinements of **1** and **2** are summarized in Table S1. CSD reference numbers, 424616 for **1** and 424618 for **2**, contain the supplementary crystallographic data for this paper. This data may be obtained from the Fachinformationszentrum Karlsruhe, 76344 Eggenstein-Leopoldshafen, Germany (fax: (+49)7247-808-666; e-mail: crysdata@fiz-karlsruhe.de).

S1 (a) A. Tézé and G. Hervé, *Inorg. Synth.*, 1990, **27**, 85; (b) J. Canny, A. Tézé and R.

Thouvenot, G. Hervé, *Inorg. Chem.*, 1986, **25**, 2114.

S2 G. M. Sheldrick, *SHELXL97, Program for Crystal Structure Refinement*, University of Göttingen: Göttingen, Germany, 1997; G. M. Sheldrick, *SHELXS97, Program for Crystal Structure Solution*, University of Göttingen: Göttingen, Germany, 1997.

Table S1 Crystal Data and Structure Refinement for **1** and **2**.

	1	2
Empirical formula	CH ₄₆ DyK ₇ Mn ₄ Na ₆ O ₉₁ Si ₂ W ₁₆	CH ₄₆ K ₁₀ Mn ₄ Na ₆ O ₉₁ Si ₂ W ₁₆
<i>M</i>	5306.06	5260.86
$\lambda/\text{\AA}$	0.71073	0.71073
<i>T</i> /K	293(2)	293(2)
Crystal dimensions/mm	0.43 × 0.12 × 0.10	0.28 × 0.20 × 0.07
Crystal system	Monoclinic	Triclinic
Space group	<i>P</i> 2(1)/ <i>c</i>	<i>P</i> -1
<i>a</i> /\AA	17.3957(15)	15.649(3)
<i>b</i> /\AA	42.861(4)	19.135(4)
<i>c</i> /\AA	12.8507(11)	19.233(4)
α°	90	62.37(3)
β°	108.4000(10)	88.04(3)
γ°	90	73.62(3)
<i>V</i> /\AA ³	9091.6(14)	4863.7(17)
<i>Z</i>	4	2
<i>D_c</i> /Mg m ⁻³	3.876	3.592
μ/mm^{-1}	21.987	19.923
<i>F</i> (000)	9428	4696
θ Range/ $^\circ$	2.51–28.39	3.00–25.00
Data/restraints/parameters	21917 / 60 / 1169	16508/228/1191
$R_1(I > 2\sigma(I))^a$	0.0387	0.0554
wR_2 (all data) ^a	0.0876	0.1479
Goodness-of-fit on F^2	0.978	1.055
^a $R_1 = \sum F_0 - F_C / \sum F_0 $; $wR_2 = \sum [w(F_0^2 - F_C^2)^2] / \sum [w(F_0^2)^2]^{1/2}$		

Table S2. Bond valence sum calculations of compounds **1** and **2**.^[S3,S4]

Bonds	Bond length (Å)	BVS	Bonds	Bond length (Å)	BVS
Compound 1			Compound 2		
Mn(1)-O(25)	1.918(7)	0.651213	Mn(1)-O(57)	1.929(13)	0.633112
Mn(1)-O(40)	1.924(8)	0.640565	Mn(1)-O(37)	1.973(13)	0.562127
Mn(1)-O(21)	1.928(7)	0.633848	Mn(1)-O(26)	1.974(14)	0.560595
Mn(1)-O(15)	1.954(7)	0.590836	Mn(1)-O(42)	2.149(16)	0.349314
Mn(1)-O(14)	2.127(8)	0.370073	Mn(1)-O(11)	2.266(12)	0.254643
Mn(1)-O(32)	2.271(7)	0.250832	Mn(1)-O(43)	1.929(13)	0.633112
$V_{\text{Mn}(1)} = 3.14$			$V_{\text{Mn}(1)} = 2.99$		
Mn(2)-O(57)	Mn(2)-O(57)	0.702406	Mn(2)-O(55)	1.914(13)	0.659306
Mn(2)-O(25)	Mn(2)-O(25)	0.645954	Mn(2)-O(57)	1.927(11)	0.636578
Mn(2)-O(20)	Mn(2)-O(20)	0.534466	Mn(2)-O(56)	1.970(14)	0.566688
Mn(2)-O(60)	Mn(2)-O(60)	0.461888	Mn(2)-O(43)	2.011(13)	0.507261
Mn(2)-O(32)	Mn(2)-O(32)	0.396049	Mn(2)-O(25)	2.118(14)	0.379862
Mn(2)-O(37)	Mn(2)-O(37)	0.327782	Mn(2)-O(63)	2.285(13)	0.24189
$V_{\text{Mn}(2)} = 3.07$			$V_{\text{Mn}(2)} = 2.99$		
Mn(3)-O(54)	1.907(7)	0.670864	Mn(3)-O(42)	1.873(15)	0.736526
Mn(3)-O(35)	1.923(8)	0.642298	Mn(3)-O(34)	1.899(15)	0.686547
Mn(3)-O(15)	1.922(7)	0.644211	Mn(3)-O(30)	1.947(14)	0.603033
Mn(3)-O(25)	1.940(7)	0.613621	Mn(3)-O(57)	1.973(13)	0.562127
Mn(3)-O(12)	2.137(8)	0.360205	Mn(3)-O(6)	2.098(13)	0.400972
Mn(3)-O(37)	2.277(7)	0.246797	Mn(3)-O(63)	2.270(11)	0.251912
$V_{\text{Mn}(3)} = 3.18$			$V_{\text{Mn}(3)} = 3.24$		
Mn(4)-O(47)	1.910(7)	0.665446	Mn(4)-O(22)	1.861(13)	0.760846
Mn(4)-O(15)	1.918(7)	0.651213	Mn(4)-O(51)	1.949(14)	0.599782
Mn(4)-O(53)	1.994(8)	0.53015	Mn(4)-O(42)	1.966(13)	0.572863
Mn(4)-O(1)	2.055(8)	0.449572	Mn(4)-O(63)	2.015(14)	0.501793
Mn(4)-O(37)	2.076(7)	0.424881	Mn(4)-O(53)	2.142(14)	0.356005
Mn(4)-O(32)	2.168(7)	0.331345	Mn(4)-O(43)	2.286(12)	0.241244
$V_{\text{Mn}(4)} = 3.05$			$V_{\text{Mn}(4)} = 3.03$		

[S3] The valence sum calculations are performed on a program of bond valence calculator, version 2.00 February **1993**, written by C. Hormillosa, with assistance from Healy, S. distributed by I. D. Brown.

[S4] I. D. Brown, Altermatt, D. *Acta Crystallogr.*, **1985**, *B41*, 244.

Section 2 Supplementary Structural Figures

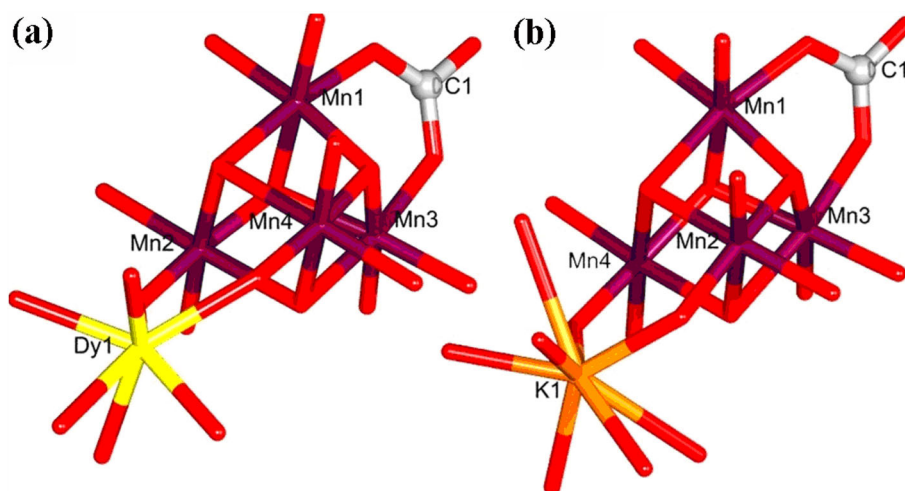


Fig. S1. (a) Ball-and-stick representation of the {DyMn₄} cluster in **1**; (b) ball-and-stick representation of the {KMn₄} cluster in **2**.

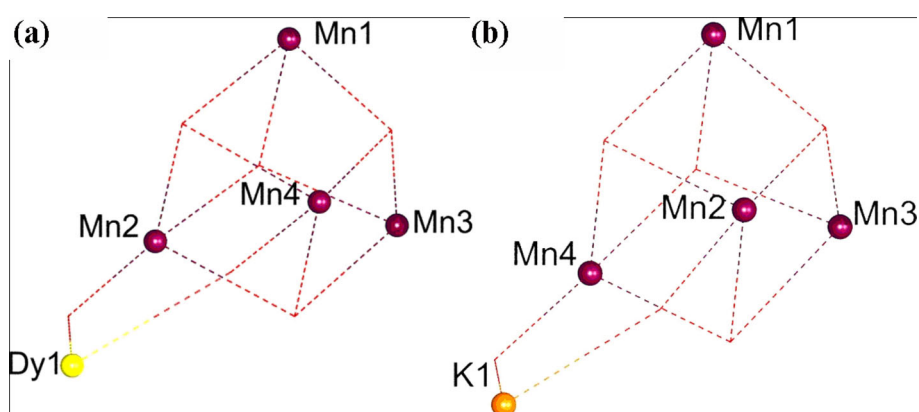


Fig. S2. (a) Appended {LnMn₄} cubane core of **1** and (b) appended {KMn₄} cubane core of **2**.

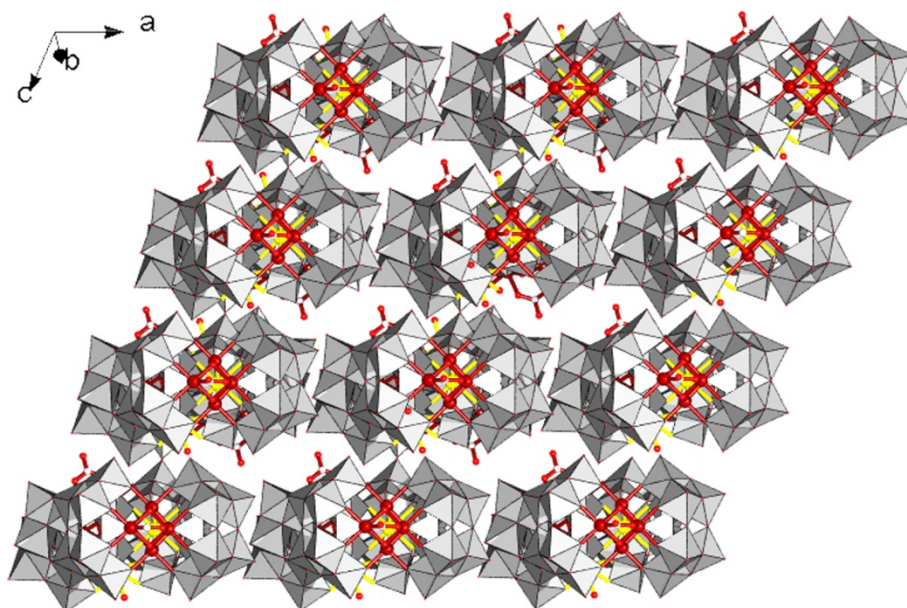


Fig. S3. The 3D packing agreement of **1** along *b*-axis. The K^+ , Na^+ and water molecules are omitted for clarity.

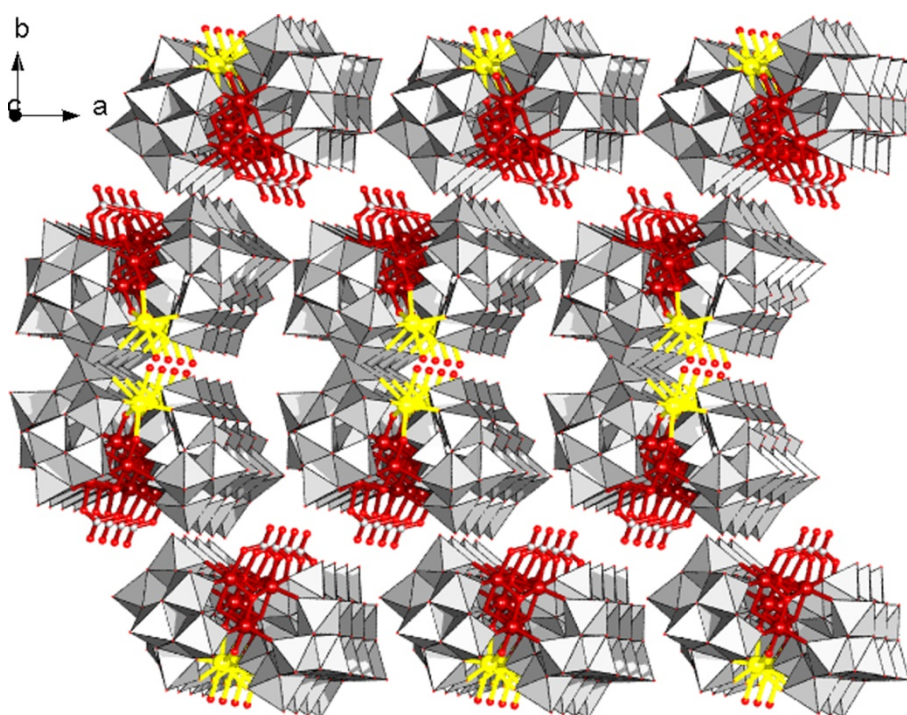


Fig. S4. The 3D packing agreement of **1** along *c*-axis. The K^+ , Na^+ and water molecules are omitted for clarity.

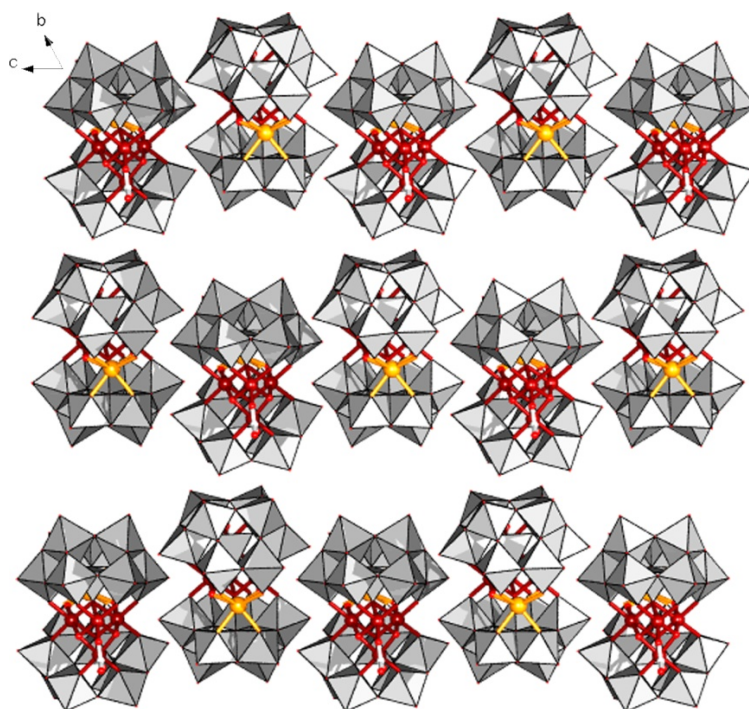


Fig. S5. The 3D packing agreement of **2** along *a*-axis. The K^+ , Na^+ and water molecules are omitted for clarity.

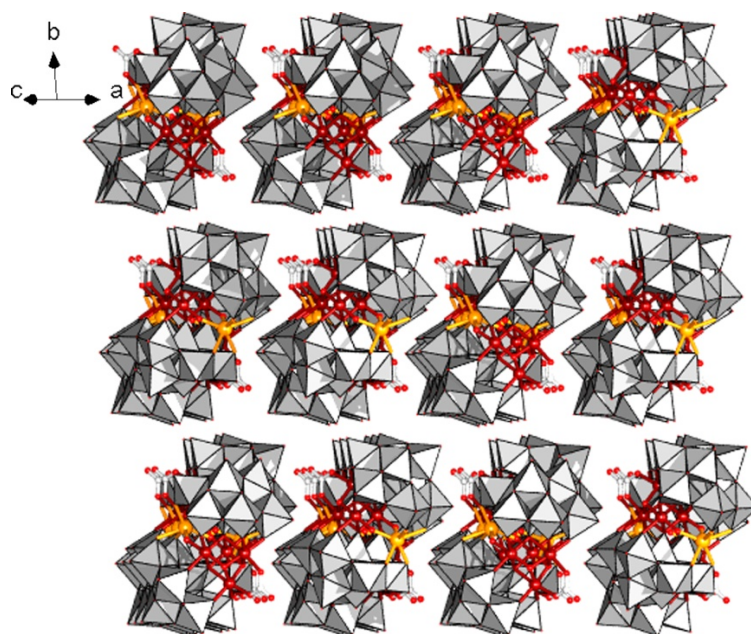


Fig. S6. The 3D packing agreement of **2**. The K^+ , Na^+ and water molecules are omitted for clarity.

Section 3 Magnetic properties

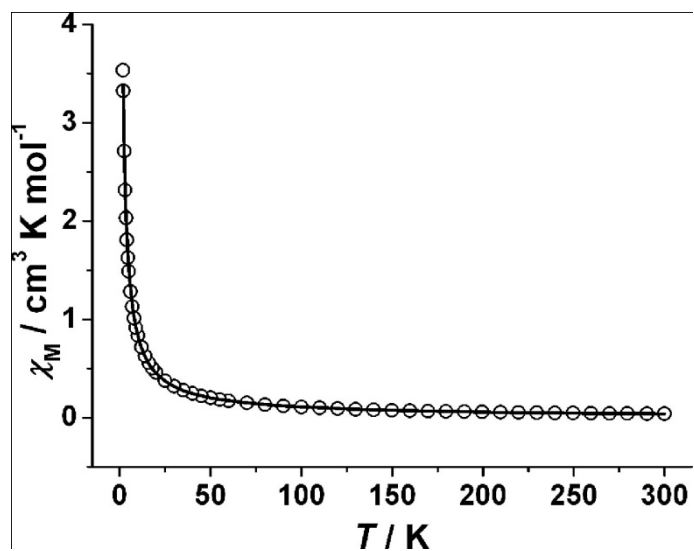


Fig. S7. Temperature dependence of magnetic susceptibilities in the form of χ_M for **2**.

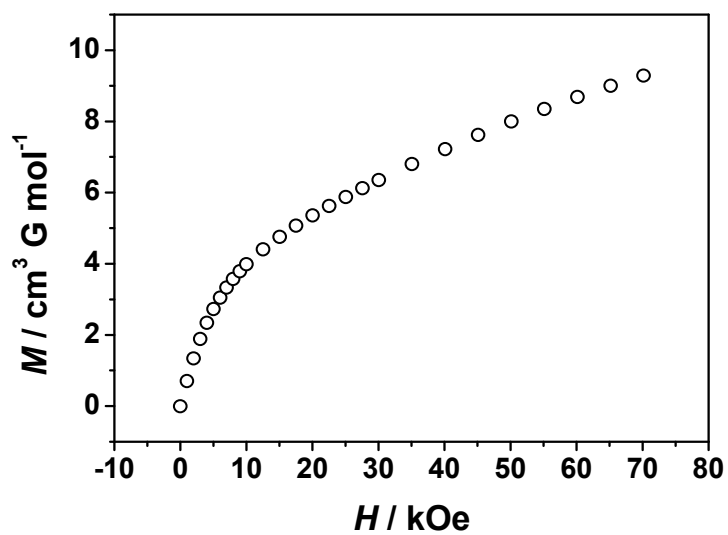


Fig. S8. Field dependence of magnetization for **2**.

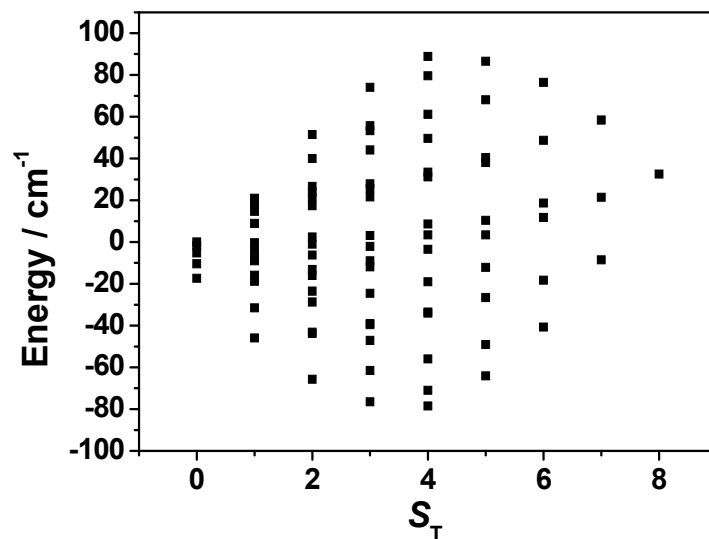


Fig. S9. The energy diagram for **2**. The energy was calculated by the fitting results J , J_1 and J_2 as described in main text.

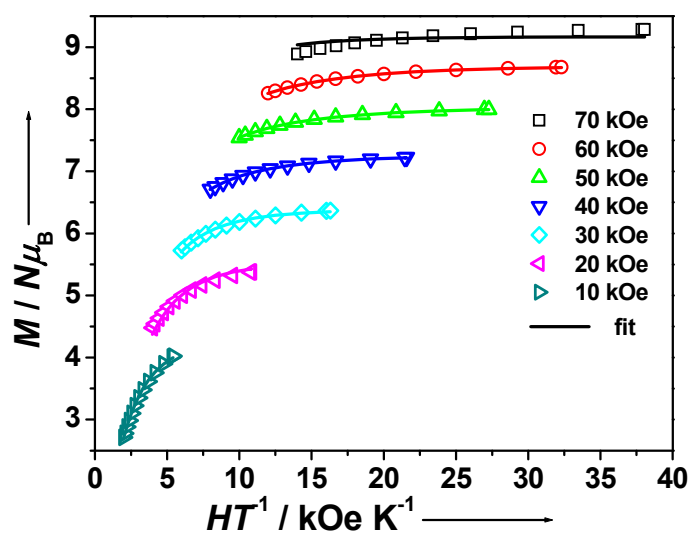


Fig. S10. Plot of reduced magnetization measurement of randomly oriented powder sample of **2** and the fit curve by ANISOFIT.

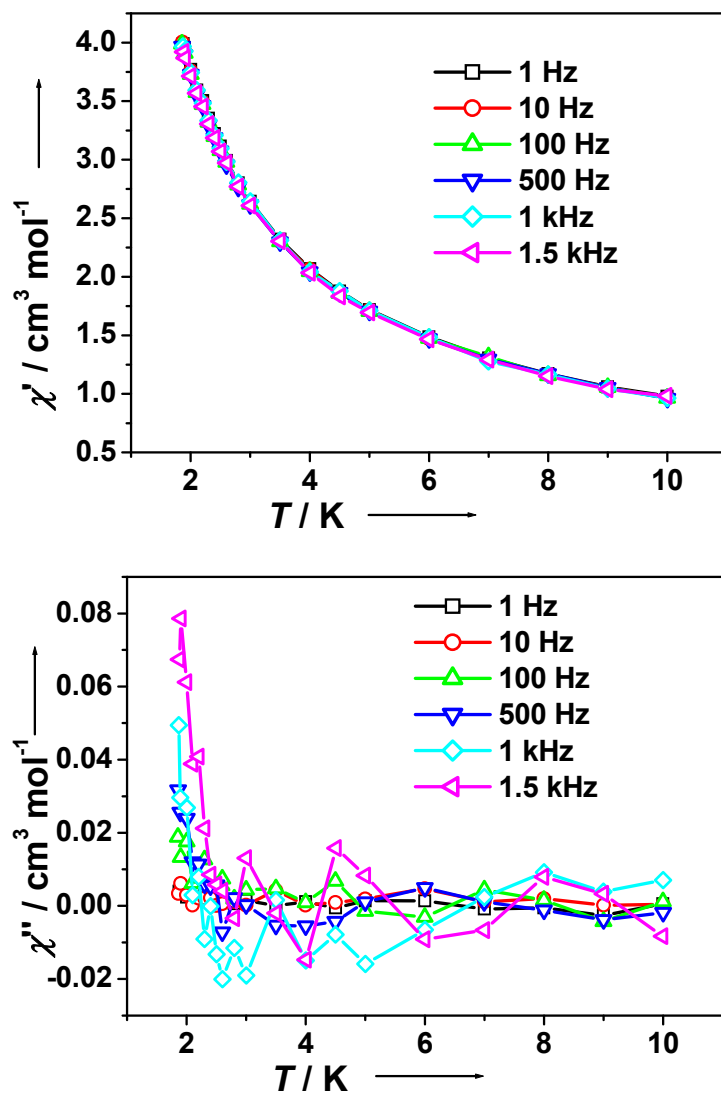


Fig. S11. Temperature dependence of the AC magnetic susceptibilities of 2.

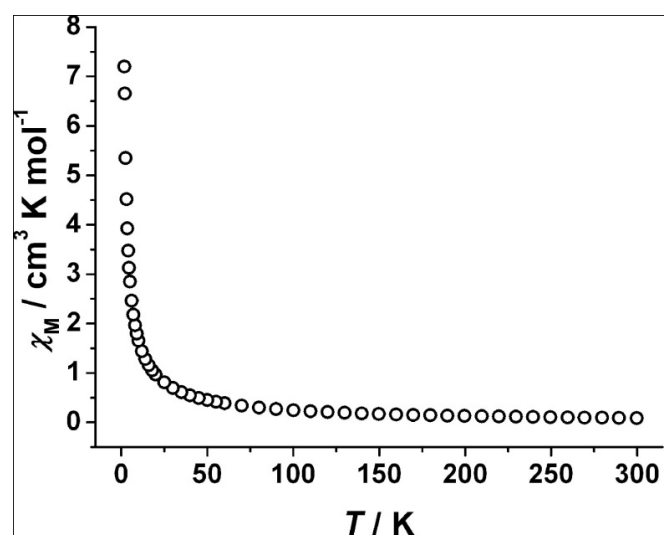


Fig. S12. Temperature dependence of magnetic susceptibilities in the form of χ_M for

1.

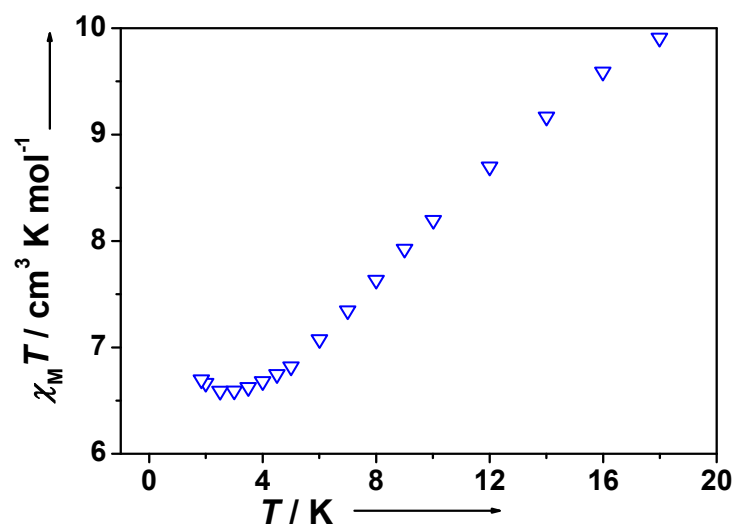


Fig. S13. Low-temperature products of $\chi_M T$ (1) - $\chi_M T$ (2).

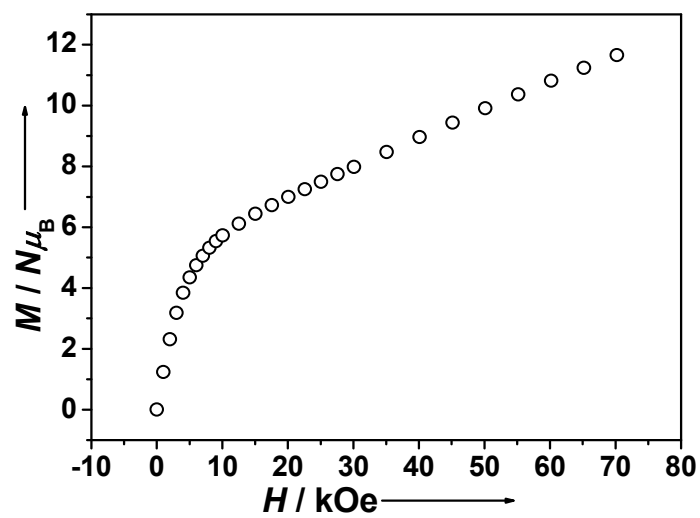


Fig. S14. Field dependence of magnetization for 1.

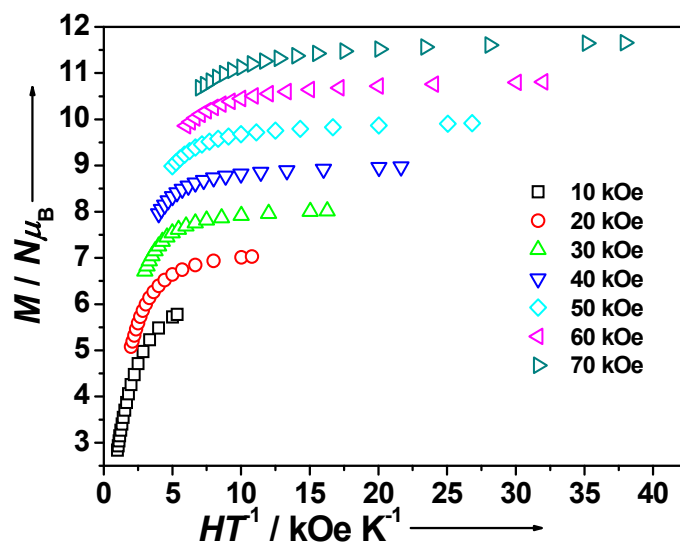


Fig. S15. Plot of reduced magnetization measurement of randomly oriented powder sample of **1**.

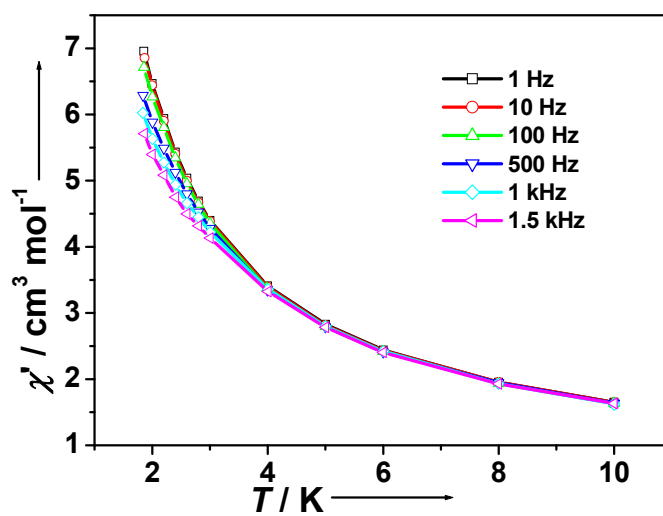


Fig. S16. Temperature dependence of the in-phase AC magnetic susceptibilities of **1** in a zero applied static field and with a 5 Oe oscillating field.

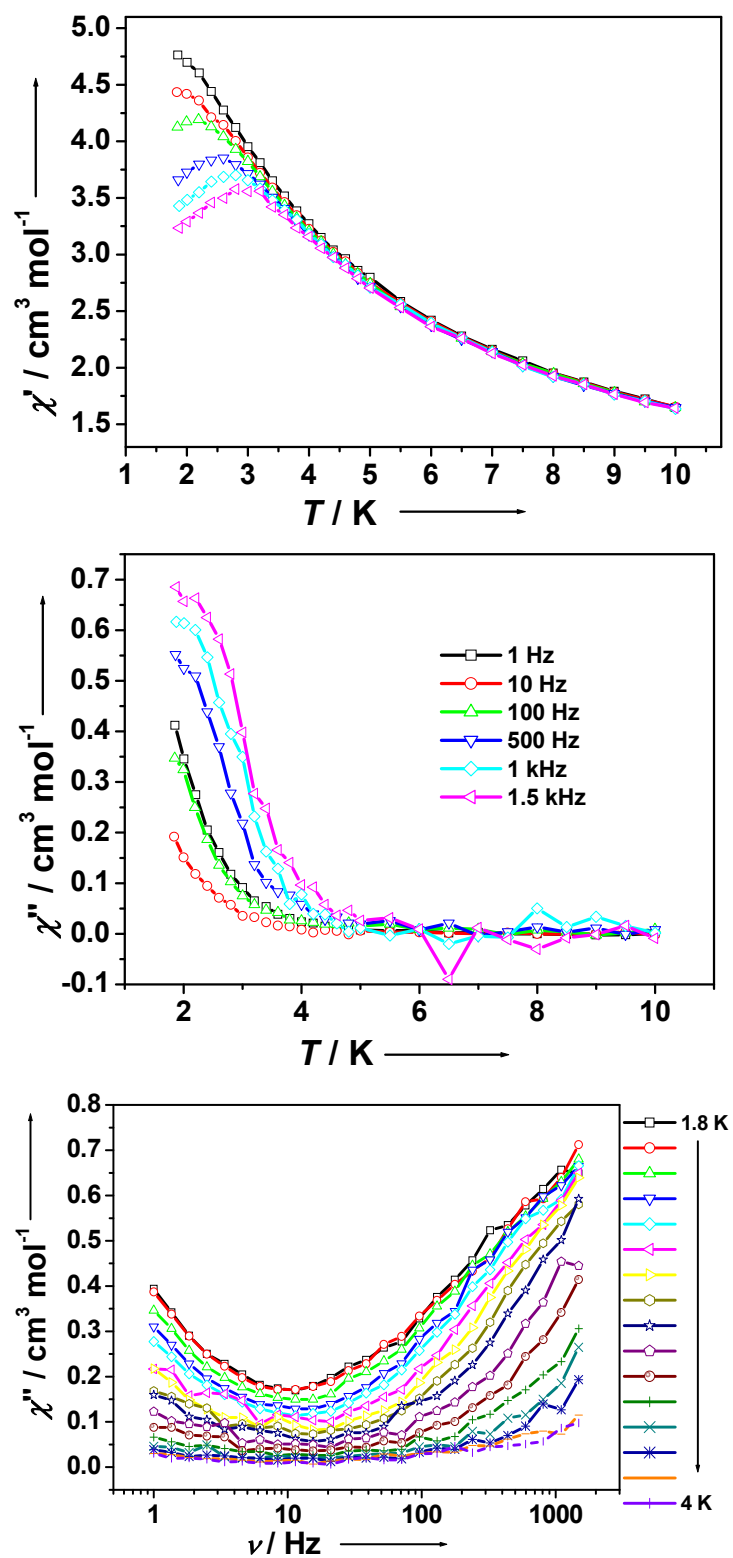
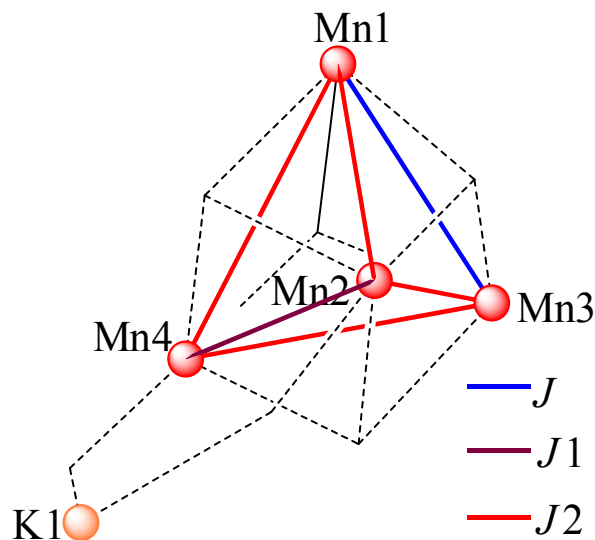


Fig. S17. Temperature dependence of the AC magnetic susceptibilities of **1** in 2 kOe applied static field and with a 5 Oe oscillating field.

Appendix: The model for fitting the magnetic properties of complex **2** by Kambe method.



$$\begin{aligned}
 \hat{H} &= -2J\hat{S}_1\hat{S}_3 - 2J_1\hat{S}_2\hat{S}_4 - 2J_2(\hat{S}_1\hat{S}_2 + \hat{S}_2\hat{S}_3 + \hat{S}_3\hat{S}_4 + \hat{S}_4\hat{S}_1) \\
 &= -2J_2[(\hat{S}_1\hat{S}_2 + \hat{S}_1\hat{S}_3 + \hat{S}_1\hat{S}_4 + \hat{S}_2\hat{S}_3 + \hat{S}_2\hat{S}_4 + \hat{S}_3\hat{S}_4) - (\hat{S}_1\hat{S}_3 + \hat{S}_2\hat{S}_4)] - 2J\hat{S}_1\hat{S}_3 - 2J_1\hat{S}_2\hat{S}_4 \\
 &= -J_2[(\hat{S}_1 + \hat{S}_2 + \hat{S}_3 + \hat{S}_4)^2 - \hat{S}_1^2 - \hat{S}_2^2 - \hat{S}_3^2 - \hat{S}_4^2] + 2J_2(\hat{S}_1\hat{S}_3 + \hat{S}_2\hat{S}_4) - 2J\hat{S}_1\hat{S}_3 - 2J_1\hat{S}_2\hat{S}_4 \\
 &= -J_2(\hat{S}_T^2 - \sum_{i=1}^4 \hat{S}_i^2) - 2(J - J_2)\hat{S}_1\hat{S}_3 - 2(J_1 - J_2)\hat{S}_2\hat{S}_4 \\
 &= -J_2(\hat{S}_T^2 - \sum_{i=1}^4 \hat{S}_i^2) - (J - J_2)[(\hat{S}_1 + \hat{S}_3)^2 - \hat{S}_1^2 - \hat{S}_3^2] - (J_1 - J_2)[(\hat{S}_2 + \hat{S}_4)^2 - \hat{S}_2^2 - \hat{S}_4^2] \\
 &= -J_2\hat{S}_T^2 + (J_2 - J)\hat{S}_A^2 + J(\hat{S}_1^2 + \hat{S}_3^2) + (J_2 - J_1)\hat{S}_B^2 + J_1(\hat{S}_2^2 + \hat{S}_4^2) \\
 &= -J_2\hat{S}_T^2 + (J_2 - J)\hat{S}_A^2 + (J_2 - J_1)\hat{S}_B^2 + J(\hat{S}_1^2 + \hat{S}_3^2) + J_1(\hat{S}_2^2 + \hat{S}_4^2)
 \end{aligned}$$

where

$$\hat{S}_A = \hat{S}_1 + \hat{S}_3, \quad \hat{S}_B = \hat{S}_2 + \hat{S}_4, \quad \hat{S}_T = \hat{S}_A + \hat{S}_B$$

$$E(S_T, S_A, S_B) = -J_2 S_T(S_T+1) + (J_2 - J)S_A(S_A+1) + (J_2 - J_1)S_B(S_B+1)$$

$$\begin{array}{ccc}
 S & \begin{array}{c} 2 \quad 2 \\ \downarrow \\ 0 \ 1 \ 2 \ 3 \ 4 \end{array} & \begin{array}{c} 2 \quad 2 \\ \downarrow \\ 0 \ 1 \ 2 \ 3 \ 4 \end{array} \\
 S_A, S_B & &
 \end{array}$$

$S_A, S_B \rightarrow S_T$

$S_A = 0$	$S_A = 1$	$S_A = 2$	$S_A = 3$	$S_A = 4$
$S_B = 0, S_T = 0$	$S_B = 0, S_T = 1$	$S_B = 0, S_T = 2$	$S_B = 0, S_T = 3$	$S_B = 0, S_T = 4$
	$S_B = 1, S_T = 1, 2$	$S_B = 1, S_T = 1, 2, 3$	$S_B = 1, S_T = 2, 3, 4$	$S_B = 1, S_T = 3, 4, 5$
$S_B = 1, S_T = 1$	$S_B = 1, S_T = 1, 2$	$S_B = 2, S_T = 1, 2, 3, 4$	$S_B = 2, S_T = 1, 2, 3, 4, 5$	$S_B = 2, S_T = 2, 3, 4, 5, 6$
$S_B = 1, S_T = 1$	$S_B = 2, S_T = 1, 2, 3, 4$	$S_B = 0, 1, 2, 3, 4$	$S_B = 3, S_T = 1, 2, 3, 4, 5, 6, 7$	$S_B = 3, S_T = 1, 2, 3, 4, 5, 6, 7$

$S_B = 2, S_T = 2$	1,2,3	$S_B = 3, S_T = 1,2,3,4,5$	0,1,2,3,4,5,6	$S_B = 4, S_T = 0,1,2,3,4,5,6,7,8$
$S_B = 3, S_T = 3$	2,3,4	$S_B = 4, S_T = 2,3,4,5,6$	$S_B = 4, S_T = 1,2,3,4,5,6,7$	
$S_B = 4, S_T = 4$	3,4,5			

(S_T, S_A, S_B)	$S_T(S_T+1)$	$S_A(S_A+1)$	$S_B(S_B+1)$	$E(S_T, S_A, S_B)$	$E_{\text{calc}} (\text{cm}^{-1})$
(0, 0, 0)	0	0	0	0	0
(1, 0, 1)	2	0	2	$-2J_1$	-7.84944
(2, 0, 2)	6	0	6	$-6J_1$	-23.5483
(3, 0, 3)	12	0	12	$-12J_1$	-47.0966
(4, 0, 4)	20	0	20	$-20J_1$	-78.4944
(1, 1, 0)	2	2	0	$-2J$	8.887
(0, 1, 1)	0	2	2	$-2J-2J_1+4J_2$	-1.7342
(1, 1, 1)	2	2	2	$-2J-2J_1+2J_2$	-0.34832
(2, 1, 1)	6	2	2	$-2J-2J_1-2J_2$	2.42344
(1, 1, 2)	2	2	6	$-2J-6J_1+6J_2$	-18.819
(2, 1, 2)	6	2	6	$-2J-6J_1+2J_2$	-16.0472
(3, 1, 2)	12	2	6	$-2J-6J_1-4J_2$	-11.8896
(2, 1, 3)	6	2	12	$-2J-12J_1+8J_2$	-43.7532
(3, 1, 3)	12	2	12	$-2J-12J_1+2J_2$	-39.5955
(4, 1, 3)	20	2	12	$-2J-12J_1-6J_2$	-34.052
(3, 1, 4)	12	2	20	$-2J-20J_1+10J_2$	-76.5368
(4, 1, 4)	20	2	20	$-2J-20J_1+2J_2$	-70.9933
(5, 1, 4)	30	2	20	$-2J-20J_1-8J_2$	-64.0639
(2, 2, 0)	6	6	0	$-6J$	26.661
(1, 2, 1)	2	6	2	$-6J-2J_1+6J_2$	14.65392
(2, 2, 1)	6	6	2	$-6J-2J_1+2J_2$	17.42568
(3, 2, 1)	12	6	2	$-6J-2J_1-4J_2$	21.58332
(0, 2, 2)	0	6	6	$-6J-6J_1+12J_2$	-5.2026
(1, 2, 2)	2	6	6	$-6J-6J_1+10J_2$	-3.81672
(2, 2, 2)	6	6	6	$-6J-6J_1+6J_2$	-1.04496
(3, 2, 2)	12	6	6	$-6J-6J_1$	3.11268
(4, 2, 2)	20	6	6	$-6J-6J_1-8J_2$	8.6562
(1, 2, 3)	2	6	12	$-6J-12J_1+16J_2$	-31.5227
(2, 2, 3)	6	6	12	$-6J-12J_1+12J_2$	-28.7509
(3, 2, 3)	12	6	12	$-6J-12J_1+6J_2$	-24.5933
(4, 2, 3)	20	6	12	$-6J-12J_1-2J_2$	-19.0498
(5, 2, 3)	30	6	12	$-6J-12J_1-12J_2$	-12.1204
(2, 2, 4)	6	6	20	$-6J-20J_1+20J_2$	-65.6922
(3, 2, 4)	12	6	20	$-6J-20J_1+14J_2$	-61.5346

(4, 2, 4)	20	6	20	$-6J-20J_1+6J_2$	-55.991
(5, 2, 4)	30	6	20	$-6J-20J_1-4J_2$	-49.0616
(6, 2, 4)	42	6	20	$-6J-20J_1-16J_2$	-40.7464
(3, 3, 0)	12	12	0	$-12J$	53.322
(2, 3, 1)	6	12	2	$-12J-2J_1+8J_2$	39.92904
(3, 3, 1)	12	12	2	$-12J-2J_1+2J_2$	44.08668
(4, 3, 1)	20	12	2	$-12J-2J_1-6J_2$	49.6302
(1, 3, 2)	2	12	6	$-12J-6J_1+16J_2$	18.68664
(2, 3, 2)	6	12	6	$-12J-6J_1+12J_2$	21.4584
(3, 3, 2)	12	12	6	$-12J-6J_1+6J_2$	25.61604
(4, 3, 2)	20	12	6	$-12J-6J_1-2J_2$	31.15956
(5, 3, 2)	30	12	6	$-12J-6J_1-12J_2$	38.08896
(0, 3, 3)	0	12	12	$-12J-12J_1+24J_2$	-10.4052
(1, 3, 3)	2	12	12	$-12J-12J_1+22J_2$	-9.01932
(2, 3, 3)	6	12	12	$-12J-12J_1+18J_2$	-6.24756
(3, 3, 3)	12	12	12	$-12J-12J_1+12J_2$	-2.08992
(4, 3, 3)	20	12	12	$-12J-12J_1+4J_2$	3.4536
(5, 3, 3)	30	12	12	$-12J-12J_1-6J_2$	10.383
(6, 3, 3)	42	12	12	$-12J-12J_1-18J_2$	18.69828
(1, 3, 4)	2	12	20	$-12J-20J_1+30J_2$	-45.9606
(2, 3, 4)	6	12	20	$-12J-20J_1+26J_2$	-43.1888
(3, 3, 4)	12	12	20	$-12J-20J_1+20J_2$	-39.0312
(4, 3, 4)	20	12	20	$-12J-20J_1+12J_2$	-33.4877
(5, 3, 4)	30	12	20	$-12J-20J_1+2J_2$	-26.5583
(6, 3, 4)	42	12	20	$-12J-20J_1-10J_2$	-18.243
(7, 3, 4)	56	12	20	$-12J-20J_1-24J_2$	-8.54184
(4, 4, 0)	20	20	0	$-20J$	88.87
(3, 4, 1)	12	20	2	$-20J-2J_1+10J_2$	74.09116
(4, 4, 1)	20	20	2	$-20J-2J_1+2J_2$	79.63468
(5, 4, 1)	30	20	2	$-20J-2J_1-8J_2$	86.56408
(2, 4, 2)	6	20	6	$-20J-6J_1+20J_2$	51.46288
(3, 4, 2)	12	20	6	$-20J-6J_1+14J_2$	55.62052
(4, 4, 2)	20	20	6	$-20J-6J_1+6J_2$	61.16404
(5, 4, 2)	30	20	6	$-20J-6J_1-4J_2$	68.09344
(6, 4, 2)	42	20	6	$-20J-6J_1-16J_2$	76.40872
(1, 4, 3)	2	20	12	$-20J-12J_1+30J_2$	20.98516
(2, 4, 3)	6	20	12	$-20J-12J_1+26J_2$	23.75692
(3, 4, 3)	12	20	12	$-20J-12J_1+20J_2$	27.91456
(4, 4, 3)	20	20	12	$-20J-12J_1+12J_2$	33.45808
(5, 4, 3)	30	20	12	$-20J-12J_1+2J_2$	40.38748
(6, 4, 3)	42	20	12	$-20J-12J_1-10J_2$	48.70276
(7, 4, 3)	56	20	12	$-20J-12J_1-24J_2$	58.40392
(0, 4, 4)	0	20	20	$-20J-20J_1+40J_2$	-17.342

(1, 4, 4)	2	20	20	$-20J-20J_1+38J_2$	-15.9561
(2, 4, 4)	6	20	20	$-20J-20J_1+34J_2$	-13.1844
(3, 4, 4)	12	20	20	$-20J-20J_1+28J_2$	-9.02672
(4, 4, 4)	20	20	20	$-20J-20J_1+20J_2$	-3.4832
(5, 4, 4)	30	20	20	$-20J-20J_1+10J_2$	3.4462
(6, 4, 4)	42	20	20	$-20J-20J_1-2J_2$	11.76148
(7, 4, 4)	56	20	20	$-20J-20J_1-16J_2$	21.46264
(8, 4, 4)	72	20	20	$-20J-20J_1-32J_2$	32.54968

$$\chi = \frac{Ng^2\beta^2}{3kT} \frac{\sum_{i=1}^6 a_i \exp(-E_i/kT)}{\sum_{i=1}^6 b_i \exp(-E_i/kT)} = \frac{Ng^2\beta^2}{3kT} \frac{\sum S_T(S_T+1)(2S_T+1) \exp[-\frac{E(S_T, S_A, S_B)}{kT}]}{\sum (2S_T+1) \exp[-\frac{E(S_T, S_A, S_B)}{kT}]}$$

$$= \frac{Ng^2\beta^2}{3kT} \frac{A}{B}$$

$$\chi_M = \frac{\chi}{1 - (2zj'/Ng^2\beta^2)\chi}$$

$$S_T = 1, S_T(S_T+1)(2S_T+1) = 6$$

$$S_T = 2, S_T(S_T+1)(2S_T+1) = 30$$

$$S_T = 3, S_T(S_T+1)(2S_T+1) = 84$$

$$S_T = 4, S_T(S_T+1)(2S_T+1) = 180$$

$$S_T = 5, S_T(S_T+1)(2S_T+1) = 330$$

$$S_T = 6, S_T(S_T+1)(2S_T+1) = 546$$

$$S_T = 7, S_T(S_T+1)(2S_T+1) = 840$$

$$S_T = 8, S_T(S_T+1)(2S_T+1) = 1224$$

$$A = 6\exp(2J_1/kT) + 30\exp(6J_1/kT) + 84\exp(12J_1/kT) + 180\exp(20J_1/kT) + 6\exp(2J/kT) + 6\exp(2J/kT + 2J_1/kT - 2J_2/kT) + 30\exp(2J/kT + 2J_1/kT + 2J_2/kT) + 6\exp(2J/kT + 6J_1/kT - 6J_2/kT) + 30\exp(2J/kT + 6J_1/kT - 2J_2/kT) + 84\exp(2J/kT + 6J_1/kT + 4J_2/kT) + 30\exp(2J/kT + 12J_1/kT - 8J_2/kT) + 84\exp(2J/kT + 12J_1/kT - 2J_2/kT) + 180\exp(2J/kT + 12J_1/kT + 6J_2/kT) + 84\exp(2J/kT + 20J_1/kT - 10J_2/kT) + 180\exp(2J/kT + 20J_1/kT - 2J_2/kT) + 330\exp(2J/kT + 20J_1/kT + 8J_2/kT) + 30\exp(6J/kT) + 6\exp(6J/kT + 2J_1/kT - 6J_2/kT) + 30\exp(6J/kT + 2J_1/kT - 2J_2/kT) + 84\exp(6J/kT + 2J_1/kT + 4J_2/kT) + 6\exp(6J/kT + 6J_1/kT - 10J_2/kT) + 30\exp(6J/kT + 6J_1/kT - 6J_2/kT) + 84\exp(6J/kT + 6J_1/kT) + 180\exp(6J/kT + 6J_1/kT + 8J_2/kT) + 6\exp(6J/kT + 12J_1/kT - 16J_2/kT) + 30\exp(6J/kT + 12J_1/kT - 12J_2/kT) + 84\exp(6J/kT + 12J_1/kT - 6J_2/kT) + 180\exp(6J/kT + 12J_1/kT + 2J_2/kT) + 330\exp(6J/kT + 12J_1/kT + 12J_2/kT) + 30\exp(6J/kT + 20J_1/kT - 20J_2/kT) + 84\exp(6J/kT + 20J_1/kT - 14J_2/kT) + 180\exp(6J/kT + 20J_1/kT - 6J_2/kT) + 330\exp(6J/kT + 20J_1/kT + 4J_2/kT) + 546\exp(6J/kT + 20J_1/kT + 16J_2/kT) + 84\exp(12J/kT) + 30\exp(12J/kT + 2J_1/kT - 8J_2/kT) + 84\exp(12J/kT + 2J_1/kT - 2J_2/kT) + 180\exp(12J/kT + 2J_1/kT + 6J_2/kT) + 6\exp(12J/kT + 6J_1/kT - 16J_2/kT) + 30\exp(12J/kT + 6J_1/kT - 12J_2/kT) + 84\exp(12J/kT + 6J_1/kT - 6J_2/kT) + 180\exp(12J/kT + 6J_1/kT + 2J_2/kT) + 330\exp(12J/kT + 6J_1/kT + 12J_2/kT) + 6\exp(12J/kT + 12J_1/kT - 22J_2/kT) + 30\exp(12J/kT + 12J_1/kT - 18J_2/kT) + 84\exp(12J/kT + 12J_1/kT - 12J_2/kT) + 180\exp(12J/kT + 12J_1/kT - 4J_2/kT) + 330\exp(12J/kT + 12J_1/kT + 6J_2/kT) + 546\exp(12J/kT + 12J_1/kT + 18J_2/kT) + 6\exp(12J/kT + 20J_1/kT - 30J_2/kT) + 30\exp(12J/kT + 20J_1/kT - 26J_2/kT) + 84\exp(12J/kT + 20J_1/kT - 20J_2/kT) + 180\exp(12J/kT + 20J_1/kT - 12J_2/kT) + 330\exp(12J/kT + 20J_1/kT - 2J_2/kT) + 546\exp(12J/kT + 20J_1/kT + 10J_2/kT) + 840\exp(12J/kT + 20J_1/kT + 24J_2/kT) + 180\exp(20J/kT) + 84\exp(20J/kT + 2J_1/kT - 10J_2/kT) + 180\exp(20J/kT + 2J_1/kT - 2J_2/kT) + 330\exp(20J/kT)$$

$$kT+2J_1/kT+8J_2/kT)+30\exp(20J/kT+6J_1/kT-20J_2/kT)+84\exp(20J/kT+6J_1/kT-14J_2/kT)+180\exp(20J/kT+6J_1/kT-6J_2/kT)+330\exp(20J/kT+6J_1/kT+4J_2/kT)+546\exp(20J/kT+6J_1/kT+16J_2/kT)+6\exp(20J/kT+12J_1/kT-30J_2/kT)+30\exp(20J/kT+12J_1/kT-26J_2/kT)+84\exp(20J/kT+12J_1/kT-20J_2/kT)+180\exp(20J/kT+12J_1/kT-12J_2/kT)+330\exp(20J/kT+12J_1/kT-2J_2/kT)+546\exp(20J/kT+12J_1/kT+10J_2/kT)+840\exp(20J/kT+12J_1/kT+24J_2/kT)+6\exp(20J/kT+20J_1/kT-38J_2/kT)+30\exp(20J/kT+20J_1/kT-34J_2/kT)+84\exp(20J/kT+20J_1/kT-28J_2/kT)+180\exp(20J/kT+20J_1/kT-20J_2/kT)+330\exp(20J/kT+20J_1/kT-10J_2/kT)+546\exp(20J/kT+20J_1/kT+2J_2/kT)+840\exp(20J/kT+20J_1/kT+16J_2/kT)+1224\exp(20J/kT+20J_1/kT+32J_2/kT)$$

$$B=1+3\exp(2J_1/kT)+5\exp(6J_1/kT)+7\exp(12J_1/kT)+9\exp(20J_1/kT)+3\exp(2J/kT)+\exp(2J/kT+2J_1/kT-4J_2/kT)+3\exp(2J/kT+2J_1/kT-2J_2/kT)+5\exp(2J/kT+2J_1/kT+2J_2/kT)+3\exp(2J/kT+6J_1/kT-6J_2/kT)+5\exp(2J/kT+6J_1/kT-2J_2/kT)+7\exp(2J/kT+6J_1/kT+4J_2/kT)+5\exp(2J/kT+12J_1/kT-8J_2/kT)+7\exp(2J/kT+12J_1/kT-2J_2/kT)+9\exp(2J/kT+12J_1/kT+6J_2/kT)+7\exp(2J/kT+20J_1/kT-10J_2/kT)+9\exp(2J/kT+20J_1/kT-2J_2/kT)+11\exp(2J/kT+20J_1/kT+8J_2/kT)+5\exp(6J/kT)+3\exp(6J/kT+2J_1/kT-6J_2/kT)+5\exp(6J/kT+2J_1/kT-2J_2/kT)+7\exp(6J/kT+2J_1/kT+4J_2/kT)+\exp(6J/kT+6J_1/kT-12J_2/kT)+3\exp(6J/kT+6J_1/kT-10J_2/kT)+5\exp(6J/kT+6J_1/kT-6J_2/kT)+7\exp(6J/kT+6J_1/kT)+9\exp(6J/kT+6J_1/kT+8J_2/kT)+3\exp(6J/kT+12J_1/kT-16J_2/kT)+5\exp(6J/kT+12J_1/kT-12J_2/kT)+7\exp(6J/kT+12J_1/kT-6J_2/kT)+9\exp(6J/kT+12J_1/kT+2J_2/kT)+11\exp(6J/kT+12J_1/kT+12J_2/kT)+5\exp(6J/kT+20J_1/kT-20J_2/kT)+7\exp(6J/kT+20J_1/kT-14J_2/kT)+9\exp(6J/kT+20J_1/kT-6J_2/kT)+11\exp(6J/kT+20J_1/kT+4J_2/kT)+13\exp(6J/kT+20J_1/kT+16J_2/kT)+7\exp(12J/kT)+5\exp(12J/kT+2J_1/kT-8J_2/kT)+7\exp(12J/kT+2J_1/kT-2J_2/kT)+9\exp(12J/kT+2J_1/kT+6J_2/kT)+3\exp(12J/kT+6J_1/kT-16J_2/kT)+5\exp(12J/kT+6J_1/kT-12J_2/kT)+7\exp(12J/kT+6J_1/kT-6J_2/kT)+9\exp(12J/kT+6J_1/kT+2J_2/kT)+11\exp(12J/kT+6J_1/kT+12J_2/kT)+\exp(12J/kT+12J_1/kT-24J_2/kT)+3\exp(12J/kT+12J_1/kT-22J_2/kT)+5\exp(12J/kT+12J_1/kT-18J_2/kT)+7\exp(12J/kT+12J_1/kT-12J_2/kT)+9\exp(12J/kT+12J_1/kT-4J_2/kT)+11\exp(12J/kT+12J_1/kT+6J_2/kT)+13\exp(12J/kT+12J_1/kT+18J_2/kT)+3\exp(12J/kT+20J_1/kT-30J_2/kT)+5\exp(12J/kT+20J_1/kT-26J_2/kT)+7\exp(12J/kT+20J_1/kT-20J_2/kT)+9\exp(12J/kT+20J_1/kT-12J_2/kT)+11\exp(12J/kT+20J_1/kT-2J_2/kT)+13\exp(12J/kT+20J_1/kT+10J_2/kT)+15\exp(12J/kT+20J_1/kT+24J_2/kT)+9\exp(20J/kT)+7\exp(20J/kT+2J_1/kT-10J_2/kT)+9\exp(20J/kT+2J_1/kT-2J_2/kT)+11\exp(20J/kT+2J_1/kT+8J_2/kT)+5\exp(20J/kT+6J_1/kT-20J_2/kT)+7\exp(20J/kT+6J_1/kT-14J_2/kT)+9\exp(20J/kT+6J_1/kT-6J_2/kT)+11\exp(20J/kT+6J_1/kT+4J_2/kT)+13\exp(20J/kT+6J_1/kT+16J_2/kT)+3\exp(20J/kT+12J_1/kT-30J_2/kT)+5\exp(20J/kT+12J_1/kT-26J_2/kT)+7\exp(20J/kT+12J_1/kT-20J_2/kT)+9\exp(20J/kT+12J_1/kT-12J_2/kT)+11\exp(20J/kT+12J_1/kT-2J_2/kT)+13\exp(20J/kT+12J_1/kT+10J_2/kT)+15\exp(20J/kT+12J_1/kT+24J_2/kT)+\exp(20J/kT+20J_1/kT-40J_2/kT)+3\exp(20J/kT+20J_1/kT-38J_2/kT)+5\exp(20J/kT+20J_1/kT-34J_2/kT)+7\exp(20J/kT+20J_1/kT-28J_2/kT)+9\exp(20J/kT+20J_1/kT-20J_2/kT)+11\exp(20J/kT+20J_1/kT-10J_2/kT)+13\exp(20J/kT+20J_1/kT+2J_2/kT)+15\exp(20J/kT+20J_1/kT+16J_2/kT)+17\exp(20J/kT+20J_1/kT+32J_2/kT)$$

Section 4. Supplementary Physical Characterizations

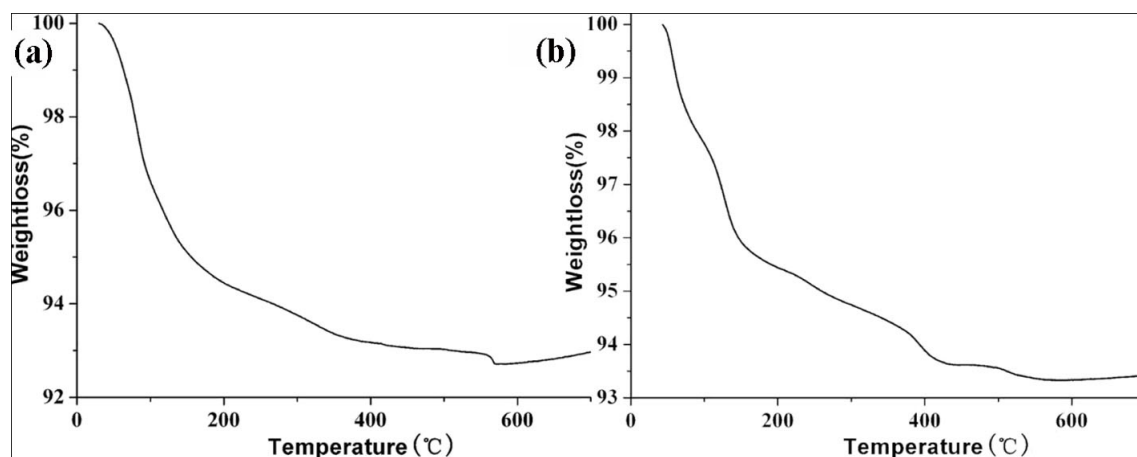


Fig. S18. (a) TGA curve of **1**. The first weight loss of 6.92 % in the range of 40 ~ 424 °C are attributed to the loss of all lattice water molecules and coordinated water molecules (calcd. 7.46%); the second weight loss at ca. 560 °C corresponds to loss of the CO_3^{2-} ions; (b) TGA curve of **2**. The first weight loss of 6.40 % in the range of 40 ~ 432 °C are attributed to the loss of all lattice water molecules and coordinated water molecules (calcd. 7.45%); the second weight loss in the range of 506 ~ 560 °C corresponds to loss of the CO_3^{2-} ions.

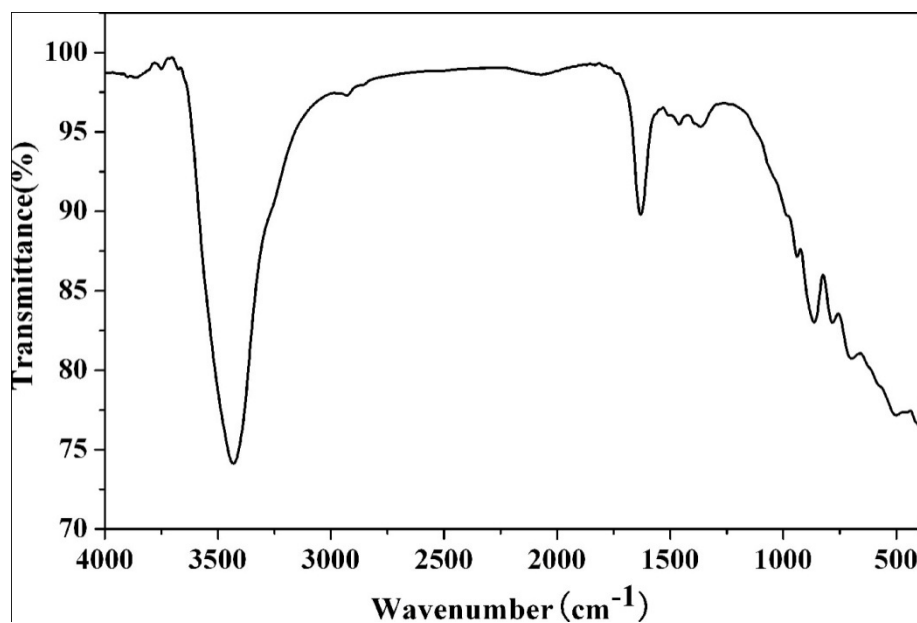


Fig. S19. IR spectrum for **1** showed the characteristic peaks of carbonate at 1461 and 1365.

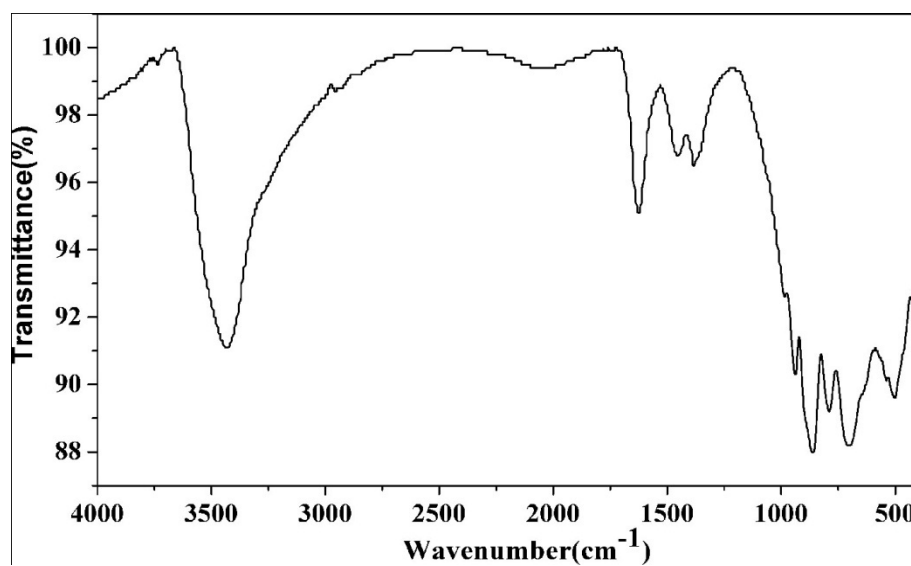


Fig. S20. IR spectrum for **2** showed the characteristic peaks of carbonate at 1459 and 1378.

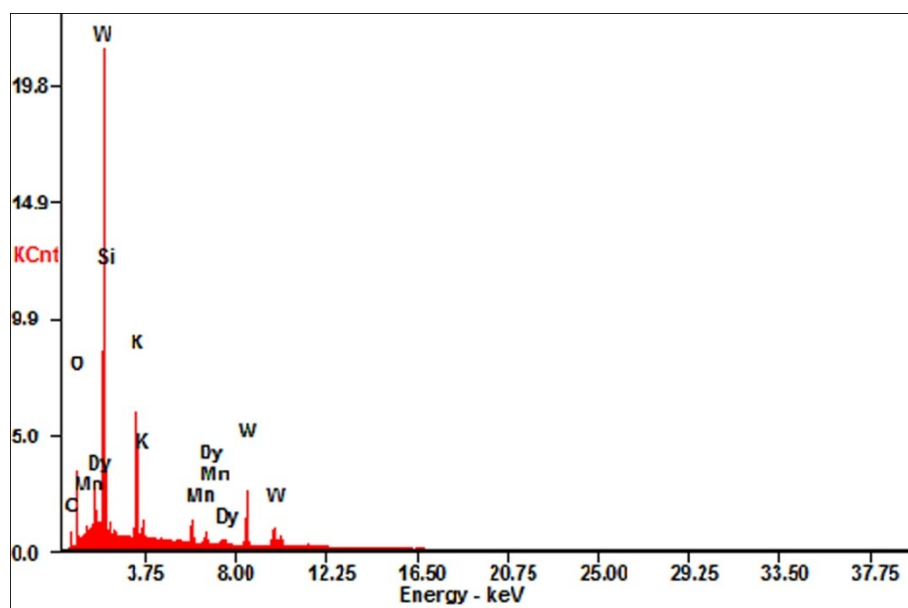


Fig. S21. Energy-dispersive X-ray (EDX) analysis of the microtube of **1**.